Folding Thermodynamics of the Hybrid-1 Type Intramolecular Human Telomeric G-Quadruplex

Folding Thermodynamics of the Hybrid-1 Type Intramolecular Human Telomeric G-Quadruplex

Yuen Lai Shek, Golamreza Dehghan Noudeh,* Mozhgan Nazari, Heiko Heerklotz, Rashid M. Abu-Ghazalah, David N. Dubins, Tigran V. Chalikian

Department of Pharmaceutical Sciences, Leslie Dan Faculty of Pharmacy, University of Toronto, 144 College Street, Toronto, Ontario, Canada M5S 3M2

ABSTRACT:

Guanine-rich DNA sequences that may form G-quadruplexes are located in strategic DNA loci with the ability to regulate biological events. G-quadruplexes have been under intensive scrutiny owing to their potential to serve as novel drug targets in emerging anticancer strategies. Thermodynamic characterization of G-quadruplexes is an important and necessary step in developing predictive algorithms for evaluating the conformational preferences of G-rich sequences in the presence or the absence of their complementary C-rich strands. We use a combination of spectroscopic, calorimetric, and volumetric techniques to characterize the folding/unfolding transitions of the 26-meric human telomeric sequence $d[A_3G_3(T_2AG_3)_3A_2]$. In the presence of K^+ ions, the latter adopts the hybrid-1 G-quadruplex conformation, a tightly packed structure with an unusually small number of solvent-exposed atomic groups. The K^+-induced folding of the G-quadruplex at room temperature is a slow process that involves significant accumulation of an intermediate at the early stages of the transition. The G-quadruplex state of the oligomeric sequence is characterized by a larger volume and compressibility and a smaller expansibility than the coil state.

These results are in qualitative agreement with each other all suggesting significant dehydration to accompany the G-quadruplex formation. Based on our volume data, 432 ± 19 water molecules become released to the bulk upon the G-quadruplex formation. This large number is consistent with a picture in which DNA dehydration is not limited to water molecules in direct contact with the regions that become buried but involves a general decrease in solute–solvent interactions all over the surface of the folded structure. © 2013 Wiley Periodicals, Inc. *Biopolymers 101: 216–227, 2014.*

Keywords: G-quadruplexes; conformational transitions; volume; compressibility; expansibility

INTRODUCTION

Guanine-rich DNA sequences that may form G-quadruplexes are located in a number of strategic DNA loci with the ability to regulate biological events. Such loci include the promoter regions of many oncogenes and the telomeric ends of eukaryotic chromosomes[1–6] Consequently, G-quadruplexes have been under intensive biochemical and biophysical scrutiny owing to their potential to serve as novel drug targets in emerging anticancer strategies.[2,6,7]

The human telomeric DNA is composed of consecutive $d(T_2AG_3)_n$ repeats with a duplex domain and a single-

Correspondence to: Tigran V. Chalikian; e-mail: chalikan@phm.utoronto.ca
*Present address: Pharmaceutics Research Center and School of Pharmacy, Kerman University of Medical Sciences, P. O. Box 76175-493, Kerman, Iran.
Y. L. Shek and G. D. Noudeh contributed equally to this work.

stranded 3'-overhang of the G-rich strand.[1,6] DNA oligomeric sequences derived from the human telomeric sequence form, *in vitro*, G-quadruplex structures that exhibit a great deal of polymorphism. The energetics of G-quadruplex polymorphism, as reflected in the conformational preferences of specific guanine-rich DNA sequences, critically depends on the stabilizing cation and the presence and the identity of flanking nucleotides.[8] In the presence of K^+ ions, human intramolecular telomeric G-quadruplexes adopt the hybrid-1 and/or hybrid-2 conformations that often exist in equilibrium.[8,9] The hybrid-1 and hybrid-2 folding topologies have been independently and practically simultaneously reported for a number of telomeric sequence varieties by several research groups.[9–14] The predominant conformation in the hybrid-1/hybrid-2 equilibrium appears to be determined by the 3'-flanking sequence.[8,9]

In a K^+ ion-rich solution, the Tel26 sequence $d[A_3G_3(T_2AG_3)_3A_2]$ overwhelmingly exists as hybrid-type (hybrid-1) intramolecular G-quadruplex consisting of three G-tetrads linked with mixed parallel/antiparallel G-strands.[8,10,11] The structure has a sequential double-chain-reversal side loop and two lateral loops each consisting of three nucleotides -TTA- thereby making the third G-strand antiparallel. The hybrid-1 G-quadruplex is specifically stabilized by the A21, A3, and A9 adenine triple capping structure that covers the top tetrad of the G-quadruplex and the A25:T14 base pair capping structure covering the bottom end.[11]

Water plays a dominant role in guiding the conformational preferences of nucleic acids, as well as in modulating and mediating nucleic acid recognition by small molecules and RNA- and DNA-binding proteins.[15–21] With respect to G-quadruplexes, water has been shown to participate in and modulate the thermodynamic stability of G-quadruplex formation, G-quadruplex polymorphism, and protein-G-quadruplex recognition.[22–26] Hence, an understanding of the interplay between various molecular forces that govern the polymorphism of G-quadruplex conformations requires a combination of structural, thermodynamic, and hydration characterizations.

In a previous work, we have applied a range of volumetric techniques to the characterization of changes in hydration accompanying the formation of Na^+-stabilized human telomeric Tel22 G-quadruplex $d[A(G_3T_2A)_3G_3]$.[27] The folding transition of Tel22 was found to be accompanied by a release of 103 ± 44 water molecules from its hydration shell to the bulk.[27] This number corresponds to $\sim 18\%$ of the net hydration of the coil conformation. In this paper, we continue our thermodynamic and hydration characterizations of G-quadruplexes. Specifically, we use a combination of volumetric, spectroscopic, and calorimetric measurements to study the K^+-stabilized hybrid-1 G-quadruplex structure formed by

$d[A_3G_3(T_2AG_3)_3A_2]$. In general, K^+-stabilized G-quadruplex structures are considered to be biologically more relevant than the Na^+-stabilized structures because of the higher intracellular concentration of potassium ions. Our analysis reveals some intriguing differences in the structural, thermodynamic, and hydration properties of the Tel22 and Tel26 G-quadruplexes, which may assist us in developing a better understanding of the conformational preferences of G-rich DNA sequences in the presence of Na^+ and K^+ ions.

RESULTS

Circular Dichroism Spectroscopy

Figure 1 (panel A) shows the CD spectrum of the oligonucleotide (ODN) in the absence of KCl and the spectra taken during the period of nine hours following the jump in KCl concentration to 30 mM. The equilibrated CD spectrum of the ODN in Figure 1a is in agreement with the CD spectrum presented by Ambrus et al.[10] in the Supplementary Material to Ref. 10. The agreement lends credence to our experimental protocols and attests to that, in the presence of potassium, the ODN adopts the hybrid-1 conformation structurally characterized by Ambrus et al.[10]

Inspection of Figure 1a reveals that the K^+-induced coil-to-quadruplex transition takes around two hours for completion. This observation is in agreement with the results of Dai et al.[9] These authors have found that, immediately after preparation, Tel26 adopts an intermediate conformation that slowly converts to the final hybrid-1 conformation.[9,10] The presence of the kinetic intermediate is corroborated by our time-dependent CD data, in particular, by the negative peak at 242 nm. As is seen from the inset in Figure 1a, the molar ellipticity at 242 nm increases immediately after the addition of KCl followed by a decrease after ~ 1 minute. This observation is consistent with the picture in which the ODN undergoes the K^+-induced coil-to-G-quadruplex transition *via* a populated intermediate at the early stages of the folding.

Further inspection of Figure 1a reveals that the slow kinetics of hybrid-1 structure formation is reflected in the positive peak at 268 nm and the negative peak at 242 nm, but not in the positive peak at the characteristic wavelength of 295 nm. The molar ellipticity at 295 nm is virtually insensitive to the folding kinetics of hybrid-1. Figure 1b shows the time dependence of the molar ellipticity at 268 nm. The kinetic profile presented in Figure 1b was measured using an ODN concentration of 23 μM. To ensure that G-quadruplex formation does not involve any aggregates, we repeated our kinetic measurements using the ODN with a 10-fold smaller concentration (2.6 μM) (data not shown). Our concentration-dependent

a)

b)
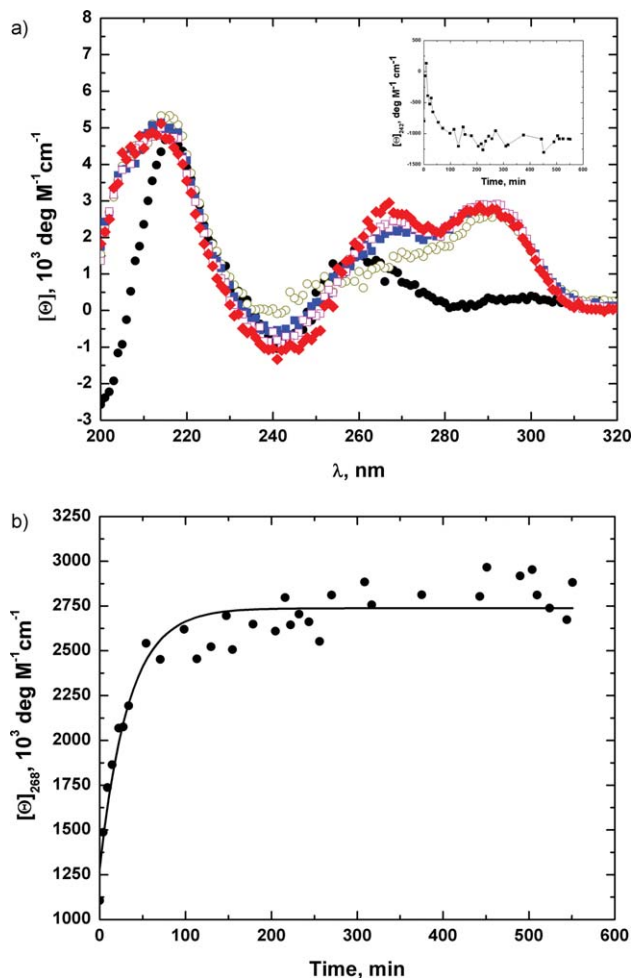
FIGURE 1 (a) CD spectra of the ODN taken in a nonfolding buffer in the absence of K^+ ions (●) and after 0 (○), 30 (■), 60 (□), and 540 (◆) min following addition of 30 mM KCl. Inset: time dependence of the molar ellipticity at 242 nm. (b) Time dependence of the molar ellipticity at 268 nm following addition of 30 mM KCl. Experimental data were approximated by an exponential function (solid line).

measurements revealed that the shapes of these kinetic profiles are independent of the concentration of the ODN. Both sets of kinetic data (at high and low concentration) can be approximated by a single exponential function $[\Theta] = [\Theta]_0 \exp(-kt)$. The values of k were 0.032 ± 0.005 and 0.040 ± 0.007 min^{-1} for the ODN concentrations of 2.6 and 23 mM, respectively. We conclude that our monitored G-quadruplex formation is a monomolecular process that does not involve aggregates.

Figure 2 plots the molar ellipticities of the ODN at 268 (panel A) and 295 (panel B) nm as a function of KCl. The aliquots of KCl were added to the DNA solution with an interval of 3 hours to allow for equilibration of the reaction of K^+-induced G-quadruplex formation. The CD titration data

have been approximated by an analytical function derived based on the following model:

$$C + nK^+ \leftrightarrow Q \qquad \text{(Reaction 1)}$$

where C collectively signifies the ensemble of coil-like conformations; Q signifies the hybrid-1 G-quadruplex conformation; and n is the number of coordinated potassium ions inside the central cavity of the G-quadruplex.

The binding constant of Reaction 1 is given by the expression:

$$K_b = \frac{[Q]}{[C][K^+]^n} = \frac{\alpha}{(1-\alpha)([K^+]_T - \alpha n[DNA])^n} \qquad (1)$$

where $[K^+]_T$ is the total concentration of potassium ions in the solution; $[DNA] = [C] + [Q]$ is the total concentrations of the ODN in solution; $[K^+]$ is the concentrations of unbound

a)

b)
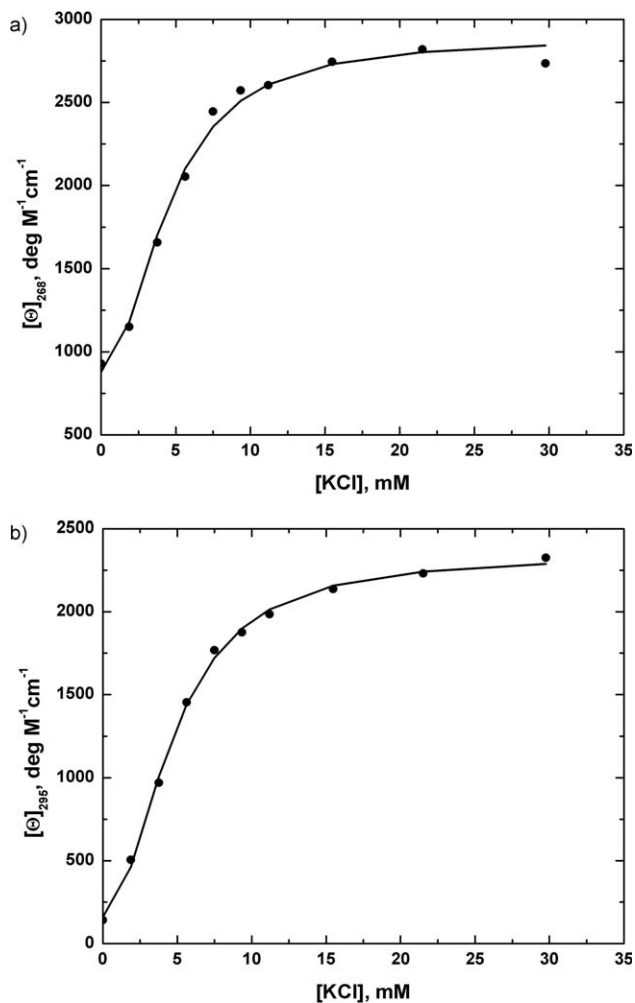
FIGURE 2 KCl dependences of the molar ellipticities of the ODN at 268 (panel A) and 295 (panel B) nm. Experimental data were approximated with Eq. (1) (solid line).

Table I   G-Quadruplex-to-Coil Transition Temperatures, T_M, and van't Hoff, δH_{vH}, and Calorimetric, δH_{cal}, Enthalpies Determined from UV Melting and DSC Measurements

[KCl], mM	T_M (UV), °C	ΔH_{vH} (UV), kcal mol^{-1}	T_M (DSC), °C	ΔH_{cal} (DSC), kcal mol^{-1}
30	55.5 ± 0.2	39.8 ± 0.5		
50	59.1 ± 0.2	41.0 ± 0.6		
75	60.6 ± 0.2	40.6 ± 0.6	60.4 ± 0.2	44.8 ± 1.1
100	62.6 ± 0.2	40.0 ± 0.7		
150	65.8 ± 0.3	41.3 ± 0.9	64.5 ± 0.3	42.2 ± 1.1
200	70.6 ± 0.3	40.6 ± 0.8		

K$^+$ ions; $\alpha = [Q]/[DNA] = [Q]/[DNA]$ is the fraction of the ODN in the G-quadruplex conformation, while $(1 - \alpha) = [C]/[DNA]$ is the fraction of the ODN in the coil conformation.

The fraction of the ODN in the G-quadruplex conformation, α, can be determined for each experimental point of the titration profile shown in Figure 2 as the ratio $\alpha = \Delta X/\Delta X_{max}$, where ΔX is the change in the experimental observable (here, molar ellipticity) relative to its initial value at [KCl] = 0; and ΔX_{max} is the asymptotic maximum change in X corresponding to the fully folded state of the ODN. We fitted the titration profile presented in Figure 2 with Eq. (1). In our analysis, we used $n = 2$, which corresponds to the structurally determined number of potassium ions coordinated by the G-quadruplex.[10] The fitting was performed numerically based on a direct search optimization technique for fitting nonlinear systems.[28] The resulting binding constant, K_b, were equal to $(50 \pm 13) \times 10^3$ and $(46 \pm 10) \times 10^3 \ M^{-2}$ for the ellipticity data at 268 and 295 nm, respectively.

UV Melting Profiles

UV melting profiles of the ODN measured at 30, 50, 75, 100, 150, and 200 mM KCl (not shown) were fitted by the analytical relationship for the two-state transition $K = (1 - \alpha^{-1})^{-1} = \exp[\Delta H_{vH}(T_M^{-1} - T^{-1})/R]$, where ΔH_{vH} is the van't Hoff enthalpy of the transition, T_M is the transition temperature, α is the fraction of the ODN that is unfolded. The latter can be calculated for each temperature from the absorption, A(T): $\alpha = [A(T) - A_N(T)]/[A_D(T) - A_N(T)]$, where $A_N(T)$ and $A_D(T)$ signify the native and denatured baselines, respectively. The values of T_M and ΔH_{vH} determined from the fit for each experimental KCl concentration are listed in Table I (columns 2 and 3, respectively).

Figure 3 plots the melting temperatures, T_M, against $\ln[K^+]$. The slope $(\delta T_M/\delta \ln[K^+])$ is proportional to the num-

ber of potassium ions, Δn_{K+}, released to the bulk upon G-quadruplex unfolding[29,30]:

$$\Delta n_{K+} = -(\Delta H_M/RT_M^2)(\partial T_M/\partial \ln[K^+]) \tag{2}$$

With the average value of ΔH_M of 45 kcal mol^{-1}, the analysis of Figure 3 with Eq. (2) yields n_{K+} of 1.5 ± 0.2. This value is within the range of similar results obtained for other G-quadruplexes.[31] Note that n_{K+} of 1.5 ± 0.2 is close to 2, the number of potassium ions coordinated to the O6 carbonyls of the guanines forming the G-quartets.[8,10] It is tempting to suggest that the release of ions accompanying the G-quadruplex unfolding transition is predominantly restricted to the ions buried inside its central cavity. This conclusion would be in agreement with the notion that the ion condensation effects are small in folding/unfolding transitions of G-quadruplexes.[32] Further studies are required for evaluating the role of the polyelectrolyte effect in the thermal stability of G-quadruplexes. Such studies are currently underway in our laboratory.

Differential Scanning Calorimetry

We performed DSC measurements at 75 and 150 mM KCl to determine the G-quadruplex-to single strand transition temperatures, T_M, and model-independent transition enthalpies, ΔH_{cal}. The comparison of the DSC-determined enthalpy, ΔH_{cal}, with the UV-determined van't Hoff enthalpy, ΔH_{vH}, enables one to judge about the presence of transition intermediates. On the other hand, the comparison of the calorimetrc T_M (DNA concentration is ~0.3 mM) with the T_M determined from UV melting experiments (DNA concentration is ~0.03 mM) enables one to judge about the presence of DNA aggregates.
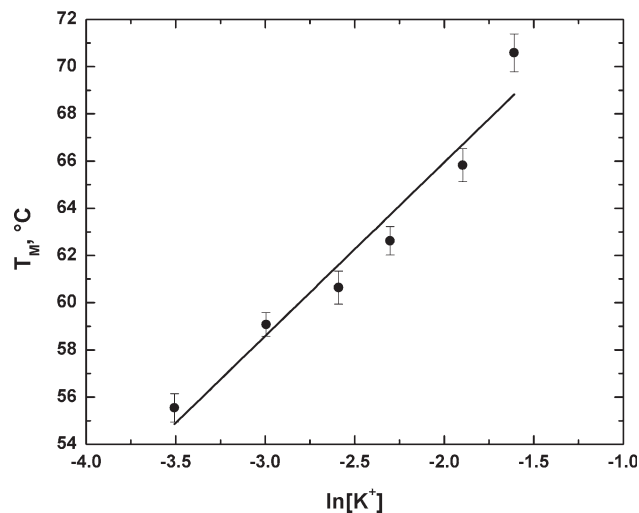
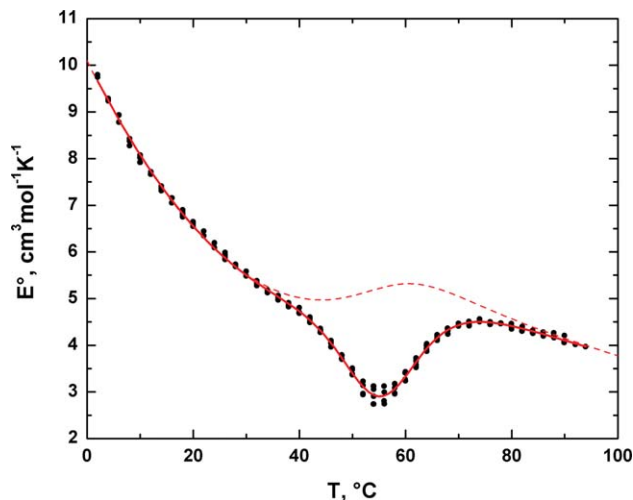**FIGURE 3**   Salt-dependence of the melting temperature.
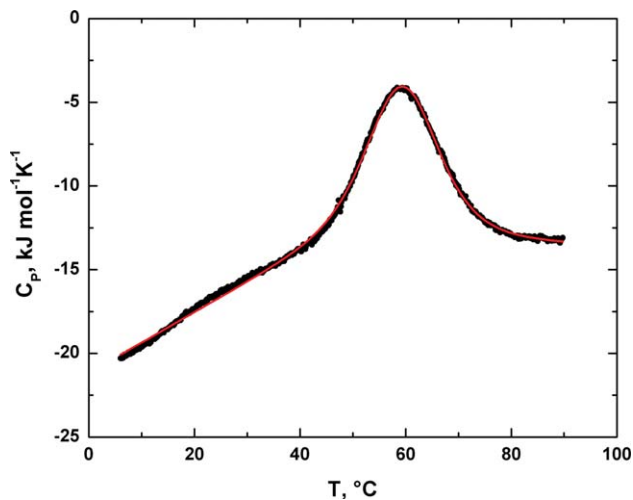
FIGURE 4 DSC thermogram of the ODN at 75 m*M* KCl. The data have been fitted (red solid line) based on the two-state approximation of thermal denaturation.

FIGURE 5 PPC melting profile of the ODN at 75 m*M* KCl. The data have been fitted (red solid line) based on the two-state approximation as described previously of thermal denaturation ([74,75]). The dashed red line is the temperature-dependent change in baseline.

Figure 4 shows a representative DSC thermogram of the ODN at 75 m*M* KCl. Inspection of Figure 4 reveals a steep predenaturational baseline. The steepness of the baseline suggests the presence of interconverting substates of the ODN all retaining their folded conformation before undergoing a cooperative unfolding transition at the transition temperature, T_M. The small shoulder observed at ~30°C, if real, may be related to the heat-induced interconversion between folded substates. The values of T_M and ΔH_{cal} determined from our DSC thermograms are listed in Table I in columns 4 and 5, respectively.

Pressure Perturbation Calorimetry

Figure 5 presents a representative PPC melting profile of the ODN at 75 m*M* KCl. Note that, in qualitative agreement with our DSC data, the PPC thermogram exhibits a steep predenaturational baseline. This result provides a further support for the temperature-induced interconversion between nearly isoenergetic yet enthalpically distinct folded subspecies of the ODN.

We used the PPC profiles to calculate the transition temperatures, T_M, and the accompanying changes in expansibility, ΔE, and in volume, ΔV_M, of the ODN. The average value of ΔE is 0.87 ± 0.24 cm³mol⁻¹K⁻¹. The values of ΔV are equal to -38.3 ± 3.7 cm³mol⁻¹ and -30.5 ± 1.5 at 75 and 150 m*M* KCl, respectively. Importantly, the PPC-determined melting temperatures, T_M (equal to 60°C and 65°C at 75 and 150 m*M* KCl, respectively), coincide with the UV- and DSC-based evaluations. The observed coincidence between the values of T_M determined by a variety of techniques on DNA samples differing in concentration by an order of magnitude lends credence to our experimental protocols while also providing support to

the monomolecular nature of the transition and the lack of aggregates.

High Precision Densimetric and Ultrasonic Velocimetric Titration Profiles

Figures 6 and 7 plot changes in volume, ΔV, and relative molar sound velocity increment, $\Delta[U]$, of the ODN at 25°C as a function of KCl concentration. We fitted the titration profiles presented in Figures 6 and 7 with Eq. (1) assuming the number of specifically bound K⁺ ions, *n*, of 2. The resulting binding constants, K_b, were equal to $(31 \pm 12) \times 10^3$ and $(25 \pm 13) \times$
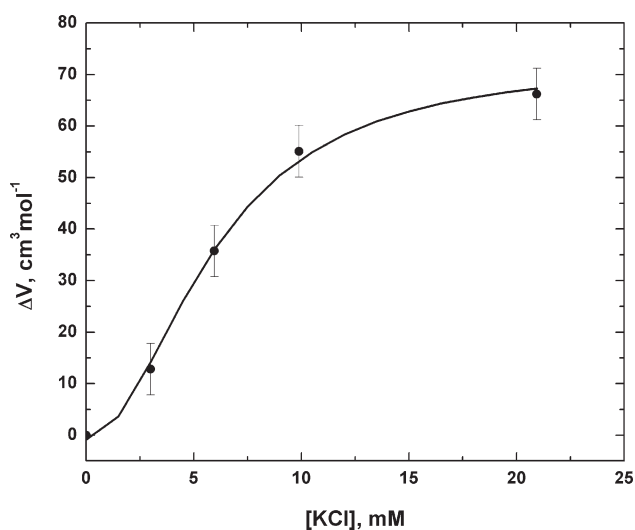
FIGURE 6 KCl dependence of the change in volume, ΔV, of the ODN at 25°C. Experimental data were approximated with Eq. (1) (solid line).
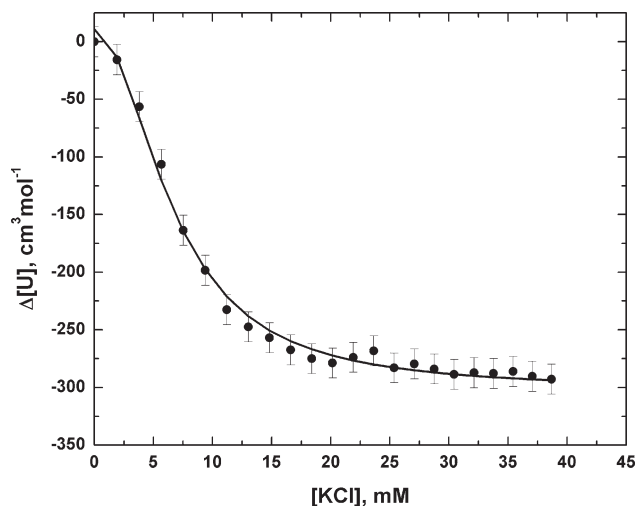
FIGURE 7 KCl dependence of the change in relative molar sound velocity increment, $\Delta[U]$, of the ODN at 25°C. Experimental data were approximated with Eq. (1) (solid line).

$10^3 M^{-2}$ for the volume (Figure 6) and sound velocity (Figure 7) data, respectively. Changes in volume, ΔV, and relative molar sound velocity increment, $\Delta[U]$, accompanying the G-quadruplex formation by the ODN are equal to 69 ± 7 cm^3mol^{-1} and -302 ± 17 cm^3mol^{-1}, respectively. It should be noted that the use in Eq. (1) of n equal to 3 or 4, while affecting the magnitude and the units of K_b, does not change significantly the values of ΔV and $\Delta[U]$. A change in adiabatic compressibility, ΔK_S, accompanying the coil-to-G-quadruplex transition is $(332 \pm 18) \times 10^{-4}$ $cm^3mol^{-1}bar^{-1}$ as calculated from $\Delta K_S = 2\beta_S°(\Delta V - \Delta[U])$ [see Eq. (7)].

Figure 8 plots the temperature dependence of the values of ΔV determined from high precision densimetric and PPC
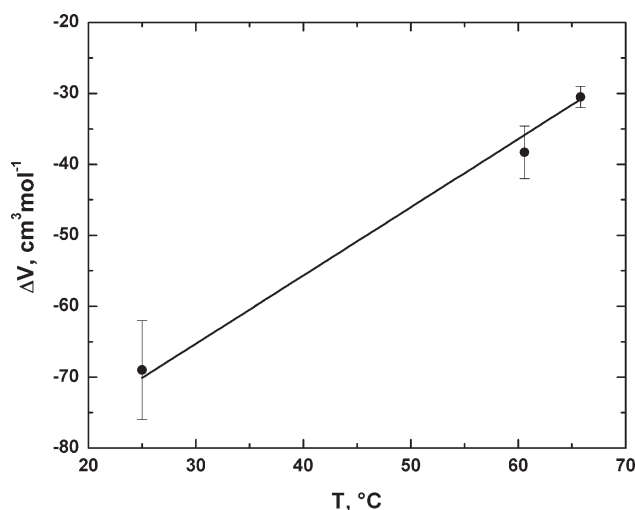

FIGURE 8 Transition volumes, ΔV, of the ODN plotted as a function of temperature.

Table II Molecular, V_M, and van der Waals, V_W, Volumes and Solvent Accessible Surface Areas, S_A, of the ODN in the Coil and Quadruplex Conformations

Conformation	S_A, Å^2	V_M, Å^3	V_W, Å^3
Coil	6311 ± 5	7086 ± 39	6245 ± 45
G-quadruplex	3963 ± 69	7092 ± 27	6066 ± 10

measurements. The slope of the dependence, which represents the change in expansibility associated with the transition, ΔE, is equal to 0.92 ± 0.07 $cm^3mol^{-1}K^{-1}$. This value is in excellent agreement with the PPC-measured ΔE of 0.87 ± 0.24 $cm^3mol^{-1}K^{-1}$.

Intrinsic Volumes and Solvent Accessible Surface Areas

Table II shows our computed van der Waals volumes, V_W, intrinsic volumes, V_M, and solvent accessible surface areas, S_A, of the ODN in the coil and G-quadruplex conformations. Inspection of Table II reveals that the coil-to-G-quadruplex transition of the ODN is accompanied by a significant decrease in solvent-accessible surface area, ΔS_A, of -2348 ± 69 Å^2 and an insignificant increase in intrinsic volume, V_M, of 6 ± 47 Å^3 $(4 \pm 28$ $cm^3mol^{-1})$.

DISCUSSION

Hybrid-1 Forms a Tightly Packed Construct with a Small Solvent-Accessible Surface Area

The structural data listed in Table II can be used to calculate the packing density, $\rho = V_W/V_M$, of the ODN in its hybrid-1 G-quadruplex conformation. We calculate a packing density, ρ, of 0.85 (6066/7092). This value (larger than the theoretical maximum for closely packed spheres of 0.74!) suggests an extremely tightly packed interior of the G-quadruplex structure despite the presence of its central hole. In fact, the presence of the central hole implies that the local packing density of hybrid-1 is even larger than 0.85.

It is instructive to compare the packing of hybrid-1 with that of the compositionally similar 22-meric human telomeric G-quadruplex d[A(G$_3$T$_2$A)$_3$G$_3$] (tel22) stabilized by a sodium ion. The intrinsic volume, V_M, of the K$^+$-stabilized 26-meric hybrid-1 is 7092 Å^3, which translates into 273 Å^3 per nucleotide (7092/26). The intrinsic volume, V_M, of Tel22 is 6426 or 293 Å^3 per nucleotide (6426/22).[27] Thus, the average volume occupied by a nucleotide in hybrid-1 is 7% smaller than that in Tel22, an observation suggesting a much tighter packing arrangement of atomic group inside hybrid-1 compared to Tel22.

Importantly, the extremely tight packing of hybrid-1 is translated into a smaller number of solvent exposed atomic groups. As is seen from Table II, the solvent-accessible surface area, S_A, of the 26-meric hybrid-1 is 3963 Å^2, which practically coincides with the value of S_A of Tel22 of 3907 Å^2.[27] This remarkable observation provides a further evidence for the compactness and extremely tight packing arrangement inside hybrid-1 suggesting that the K$^+$-stabilized 26-meric G-quadruplex exposes the same number of atomic groups to the solvent as does the Na$^+$-stabilized 22-meric G-quadruplex.

It is reasonable to speculate that the tighter packing of hybrid-1 results in stronger interatomic interactions inside its water-inaccessible core relative to those of Tel22. It is yet to be seen if the tighter packing of K$^+$-stabilized G-quadruplexes relative to that of Na$^+$-stabilized G-quadruplexes is a general trend and if it contributes to the higher stability of K$^+$-stabilized structures. The present study is the first step in that direction.

Hybrid-1 Melting is not Accompanied by a Significant Change in Heat Capacity

Comparison of the two sets of enthalpic data (calorimetric enthalpy and optically determined van't Hoff enthalpy) in Table I reveals a close agreement between the calorimetric, ΔH_{cal}, and van't Hoff, ΔH_{vH}, enthalpies. In the absence of fortuitous compensations, this agreement may suggest that the thermally induced unfolding of hybrid-1 is a two-state process. This notion contrasts results of a number of studies which suggest that the heat-induced G-quadruplex-to-coil unfolding transitions of human telomeric sequences involve populated intermediates.[33–36] However, as has been shown by Olsen et al.,[31]), the nature of G-quadruplex unfolding transition depends on the individual G-quadruplex; it may proceed either as a two-state transition or may involve intermediates. More detailed studies are required to determine the nature of the heat-induced unfolding transition of hybrid-1.

Further inspection of data listed in Table I suggests lack of dependence of the optically or calorimetrically measured transition enthalpies, ΔH, on the melting temperature, T_M. This observation is consistent with the picture in which the heat-induced unfolding transition of hybrid-1 proceeds without any considerable change in heat capacity, ΔC_P. This result contrasts one study that reports significant changes in heat capacity to accompany melting transitions of G-quadruplexes.[37]

Heat-Induced G-quadruplex-to-Coil Transition Results in a Decrease in Volume and an Increase in Expansibility

Based on our PPC results (see Figure 5), the coil state of the ODN exhibits a lower volume and a higher expansibility relative to the folded G-quadruplex state. These observations parallel our volume and expansibility results previously obtained on the Na$^+$-stabilized Tel22 G-quadruplex.[27] It is tempting to speculate that a larger partial molar volume relative to the coil state is a volumetric signature of a G-quadruplex. However, as discussed below in the section that follows, a change in volume accompanying G-quadruplex formation contains contributions of opposite signs. At present, in the absence of volumetric databases on structurally distinct G-quadruplexes, it is difficult to judge the validity and/or generality of a positive ΔV of G-quadruplex formation. Clearly, further studies are required to support or refute this speculation.

A larger partial molar expansibility, $E°$, of the coil state relative to the G-quadrupex state is indicative of more extensive hydration of the former, since all atomic groups are characterized by a positive hydration contribution to the partial molar expansibility of a solute.[38] However, it is not a trivial matter to quantify changes in hydration based on our measured value of ΔE. A change in expansibility associated with G-quadruplex formation is given by the sum:

$$\Delta E = \Delta E_M + \Delta E_h + \Delta E_{rel} - nE_{K+} \qquad (3)$$

where ΔE_M is the change in the intrinsic expansibility of the ODN; ΔE_h is the change in expansibility due a change in DNA hydration; E_{K+} is the partial molar expansibility of a potassium ion; and ΔE_{rel} is the change in the relaxation contribution, $E_{rel} = (<\Delta H \Delta V> - <\Delta H><\Delta V>)/RT^2$, $<\Delta H>$ and $<\Delta V>$ are, respectively, the ensemble average changes in enthalpy and volume relative to a "ground state" conformation.[39]

Currently, it is complicated to evaluate a change in the intrinsic expansibility, ΔE_M, of the ODN accompanying its folding/unfolding transition. While the intrinsic expansibility, E_M, of the coil state is probably close to zero, that of the folded state with its expandable voids may be quite significant. A change in the relaxation component of the partial molar expansibility, ΔE_{rel}, also may be quite significant, as emphasized in our previous publication.[27] It is difficult to come up with a valid *a priori* estimate of not only the magnitude but even the sign of ΔE_{rel}. The relaxation component mostly originates from the existence of a broadly distributed isoenergetic population of unfolded, coil-like conformations differing in enthalpy and volume. An increase in temperature shifts the population of coil-like conformations towards the species with a greater enthalpy, which would result in a positive or negative value of ΔE_{rel} depending on the sign of the volume difference between the high and low enthalpy subpopulations.

Volume Data Suggest that 432 Waters are Released upon the Coil-to-G-quadruplex Transition

We use our measured change in volume to evaluate the number of water molecules released to the bulk upon G-quadruplex formation. To this end, we use an approximate algorithm that has been described earlier.[27] A change in volume associated with G-quadruplex formation, ΔV, can be presented as the sum:

$$\Delta V = \Delta V_M + \Delta V_T + \Delta V_I - nV_{K+} \qquad (4)$$

where ΔV_M is the change in the molecular volume of the ODN (geometric volume impenetrable to water molecules); ΔV_T is the change in thermal volume; ΔV_I is the change in interaction volume; and $V_{K+} = 4.3$ cm^3mol^{-1} is the partial molar volume of a potassium ion.[40] As mentioned above, we use in our analyses $n = 2$ corresponding to the structurally determined number of potassium ions coordinated by the G-quadruplex.

Thermal volume, V_T, results from mutual vibrations of solute and solvent molecules and steric and structural effects reflecting imperfect packing of solute and solvent molecules and the open structure of water.[41,42] As a first approximation, a change in thermal volume can be calculated by multiplying the change in solvent-accessible surface area, ΔS_A, by the effective thickness of thermal of volume, δ.

We used structural data (PDB entry 2HY9) and the standard calculation procedures to compute the molecular volume, V_M, and solvent accessible area, S_A, of the ODN in its G-quadruplex conformation.[43–46] The values of V_M and S_A calculated as averages for the 10 NMR-based structural models of the telomeric oligonucleotide $d[A_3(G_3T_2A)_3G_3A_3]$[47] are 7092 ± 27 $Å^3$ (4271 ± 16 cm^3mol^{-1}) and 3963 ± 59 $Å^2$, respectively (see Table II). As described in Materials and Methods, we employed molecular dynamics (MD) simulations to generate unfolded structures beginning from the stacked, fully helical conformation. Based on these simulations, we selected the conformations exhibiting the highest and the lowest solvent accessible surface areas and calculated V_M of 7086 ± 39 $Å^3$ (4267 ± 23 cm^3mol^{-1}) and S_A of 6311 ± 5 $Å^2$ as the average values for the two coil conformations (see Table II). Thus, changes in molecular volume, ΔV_M, and solvent accessible surface area, ΔS_A, accompanying the coil-to-G-quadruplex transition are equal to 6 ± 47 $Å^3$ (4 ± 28 cm^3mol^{-1}) and -2348 ± 69 $Å^2$, respectively.

Our analysis critically depends on the assumed value of the thickness of the thermal volume, δ. This is not a trivial matter as there have been various empirical and theoretical estimates of the thickness of the empty layer, δ, reported in the literature.[41,42,48–51] For low molecular weight molecules, the different estimates of δ are in good agreement with each other,

being within a range of 0.4–0.6 Å.[41,42,52] However, the values of δ reported for larger molecules approaching the size of proteins diverge significantly, ranging from 0.226 to 1.0 Å.[48–50] In fact, our recent MD simulations-based study has revealed that the thickness of thermal volume, δ, may vary between $\sim$0.5 and $\sim$1.0 Å in a manner that depends on the size of a solute.[52] In our derivations below, we use the value of δ of 0.5 Å that has been used for DNA analysis in our previous publications.[27,53] While this is a reasonable value, one should be aware of its influence on our estimate of a change in hydration accompanying G-quadruplex formation (see below). The situation may complicate even further given the unexplored possibility of the differential value of δ for the folded and unfolded states of the ODN. Additional theoretical and computational studies are needed to better substantiate the choice of α of a DNA as function of its conformational state. For the moment, with our assumed value of δ of 0.5 Å, we calculate a change in thermal volume $\Delta V_T = \delta\Delta S_A$ of $0.5 \times (-2348 \pm 69) = -1174 \pm 35$ $Å^3$ (-707 ± 21 cm^3mol^{-1}).

At 25°C, the measured change in volume accompanying the coil-to-quadruplex transition, ΔV, is 69 ± 7 cm^3mol^{-1}. With this value, we use Eq. (4) to calculate a change in the interaction volume; $\Delta V_I = 69 - 6 + 707 + (2 \times 4.3) = 779 \pm 35$ cm^3mol^{-1}.

A change in interaction volume, $\Delta V_I = \Delta n_h(V_h - V_0)$, in Eq. (4) is determined by the number of water molecules released to the bulk, Δn_h, and the average differential partial molar volume of water of solute hydration and bulk water, $(V_h - V_0)$. For proteins and nucleic acids, the partial molar volume of water of hydration, V_h, is $\sim$10% smaller than that of bulk water, V_0.[53] With $(V_h - V_0) = -1.8$ cm^3mol^{-1}, the number of water molecules, $\Delta n_h = -\Delta V_I/(V_h - V_0)$, released to the bulk upon quadruplex formation is 432 ± 19 (779/1.8). The number of water molecules released to the bulk from the first coordination layer of the oligonucleotide is $\sim$261 as calculated by dividing ΔS_A by 9 $Å^2$, the effective cross-sectional area of a water molecule. This number is $\sim$60% smaller than our estimate of Δn_h of 432 ± 19. The disparity is consistent with a picture in which DNA dehydration associated with G-quadruplex formation is not localized. The dehydration is not limited to water molecules in direct contact with the regions of the DNA that become buried, but involves a general decrease in solute–solvent interactions all over the surface of the folded structure.

Compressibility Data Suggest a Decrease in Hydration to Accompany G-quadruplex Formation

Charged solutes, including nucleic acids, exhibit highly negative partial molar adiabatic compressibilities.[54–60] This observation reflects the fact that waters solvating charged groups are

characterized by a smaller partial molar adiabatic compressibility relative to that exhibited by bulk water.[54,56–58,60] Thus, a large increase in adiabatic compressibility, ΔK_S, of $(332 \pm 18) \times 10^{-4}$ cm^{3}mol^{-1}bar^{-1} is consistent with significant dehydration of the ODN accompanying its folding transition. In this respect, the compressibility data are in qualitative agreement with our volume and expansibility results.

More rigorously, a change in adiabatic compressibility accompanying G-quadruplex formation can be presented as the sum of the following contributions:

$$\Delta K = \Delta K_M + \Delta\Delta K_h + \Delta K_{rel} - nK_{K+} \quad (5)$$

where ΔK_M is the change in the intrinsic compressibility of the ODN; $\Delta\Delta K_h$ is the contribution arising from the differential hydration of the coil and G-quadruplex states; $K_{rel} = (<\Delta V^2> - <\Delta V>^2)/RT$ is the relaxation contribution to compressibility; and $K_{K+} = -26.5 \times 10^{-4}$ cm^{3}mol^{-1}bar^{-1} is the partial molar adiabatic compressibility of a potassium ion.[61]

The hydration contribution is given by $\Delta\Delta K_h = \Delta n_h(K_h - K_0)$, where $(K_h - K_0)$ is the difference in partial molar adiabatic compressibilities between water of solute hydration and bulk water. In principle, the contribution $\Delta\Delta K_h$ can be used to quantify the change in ODN dehydration associated with its G-quadruplex formation. However, as was the case with expansibility, the hydration contribution to compressibility, $\Delta\Delta K_h$ is difficult to evaluate from the measured value of ΔK_S because of the unknown intrinsic, ΔK_M, and relaxation, ΔK_{rel}, contributions.

The intrinsic compressibility of single and double stranded DNA is negligible,[54,60,62,63]), whereas the intrinsic compressibility of the G-quadruplex can be significant given the bulkiness of the structure and the presence of the central cavity. Consequently, a positive change in intrinsic compressibility, ΔK_M, is expected to accompany a coil-to-quadruplex transition. The relaxation contribution to compressibility, ΔK_{rel}, results from the pressure-induced shift in the ensemble population of solute molecules towards the species with smaller partial molar volume. As shown previously, the value of ΔK_{rel} can be quite significant for the folding/unfolding transitions of G-quadruplexes.[27]

CONCLUDING REMARKS

We used a combination of spectroscopic, calorimetric, and volumetric techniques to characterize the folding/unfolding transitions of the 26-meric oligonucleotide (ODN) d[A$_3$G$_3$(T$_2$AG$_3$)$_3$A$_2$] which, in the presence of K$^+$ ions, adopts the hybrid-1 G-quadruplex conformation. The latter forms an extremely tightly packed structure with an unusually small

number of atomic groups exposed to solvent as suggested by our analysis of the structural NMR data on the G-quadruplex. Our CD data reveal that, at room temperature, the K$^+$-induced folding of the ODN is a slow process that proceeds with a significant accumulation of a kinetic intermediate at the early stages of folding transition. The G-quadruplex state of the ODN is characterized by a larger volume and compressibility and a smaller expansibility than the coil state. These results are in qualitative agreement with each other all suggesting significant dehydration to accompany the G-quadruplex formation. Based on our volume data in conjunction with structural data, we estimate that 432 ± 19 water molecules become released to the bulk upon the G-quadruplex formation. This large number is consistent with a picture in which DNA dehydration is not limited to water molecules in direct contact with the regions that become buried but involves a general decrease in solute-solvent interactions all over the surface of the folded structure.

MATERIALS AND METHODS

Materials

The oligodeoxyribonucleotide (ODN), d[A$_3$(G$_3$T$_2$A)$_3$G$_3$A$_2$], containing four repeats of the human telomeric DNA sequence was synthesized and cartridge purified by ACGT (Toronto, ON, Canada). Potassium chloride, phosphoric acid, and tetrabutylammonium hydroxide 30 hydrate were purchased from Sigma-Aldrich Canada (Oakville, ON, Canada). EDTA (free acid) was purchased from Fisher Biotech (Fair Lawn, NJ, USA). These reagents were of the highest grade commercially available and used without further purification. All solutions were prepared using doubly distilled water.

To ensure the initial unfolded conformation of the oligonucleotide for high precision densimetric, ultrasonic velocimetric, and circular dichroism (CD) titration experiments, the DNA was dissolved in and dialyzed against a nonfolding buffer consisting of 10 mM tetrabutylammonium phosphate titrated to pH 7.0 and 0.1 mM EDTA. Given their large size, tetrabutylammonium cations do not stabilize quadruplex structures. The titrations were carried out with the same buffer into which KCl was added at concentrations ranging between 0.2 and 1 M.

For UV melting, differential scanning calorimetric (DSC), and pressure perturbation calorimetric (PPC) temperature scanning experiments, the ODN was dissolved in and exhaustively dialyzed against a pH 7.0 buffer consisting of 10 mM potassium phosphate, 0.1 mM EDTA, and KCl at a desired concentration. To form the equilibrium structure, the DNA-containing solution was placed in a boiling water bath and allowed to cool to room temperature. Dialysis was carried out in 1000 Da molecular weight cutoff Tube-O-Dialyzers from G Biosciences (St. Louis, MO, USA). The final dialysis buffer was retained and used for DSC and PPC experiments.

The concentration of the ODN was determined from the absorbance at 260 nm measured at 25°C with a Cary 300 Bio spectrophotometer (Varian Canada, Mississauga, ON, Canada) using a molar extinction coefficient of $278{,}200 M^{-1}$ cm^{-1} for the unfolded

conformation. The extinction coefficient was calculated using an additive nearest neighbor procedure as described by Dr. Richard Owczarzy (http://www.owczarzy.net/extinct.htm). For the DSC, PPC, densimetric, and ultrasonic velocimetric experiments, DNA concentrations were on the order of ~0.3 mM. For CD measurements and temperature-dependent UV light absorption measurements, the DNA concentrations were ~0.05 and ~0.03 mM, respectively.

Circular Dichroism Spectroscopy

The CD spectra of the ODN were recorded in a 1 mm path-length cuvette at 25°C using an Aviv model 62 DS spectropolarimeter (Aviv Associates, Lakewood, NJ). CD spectroscopy was used prior to each ultrasonic and densimetric titration to confirm that the DNA was in a coil conformation.

In CD titration experiments, CD spectra were measured following a 3 hours wait after each addition of an aliquot of potassium chloride to a cuvette containing a known amount of DNA (initially, in the coil form in the absence of K$^+$ ions). In kinetic experiments, the spectra were recorded every minute during the first 5 minutes and every 5 minutes thereafter during the 10 hours after the addition to the coil-state DNA solution of an aliquot of KCl that brought its final concentration to 30 mM.

UV Melting Experiments

UV light absorption at 295 nm was measured as a function of temperature in a DNA sample contained in a 1 cm path-length cuvette. These measurements were performed by a Cary 300 Bio spectrophotometer (Varian Canada, Mississauga, ON, Canada). The temperature was changed at a rate of 1°C/min. The G-quadruplex-to-coil transition temperatures, T_M, and van't Hoff enthalpies, ΔH_{vH}, were evaluated from our experimental UV melting profiles using standard procedures (Marky & Breslauer, 1987; Breslauer, 1994).

Differential Scanning Calorimetry

Calorimetric melting experiments on the G-quadruplex were performed at a scan rate of 1°C/min using a Microcal VP-DSC differential scanning calorimeter (MicroCal, LLC, Northampton, MA). The measurements were performed at 75 and 150 mM KCl. DNA concentrations were on the order of 120 mM (~1 mg/mL). Appropriate buffer *versus* buffer baselines were determined prior to and immediately after the oligomer *versus* buffer scan and averaged. After subtraction of the buffer scan, the DNA scan was normalized for concentration and analyzed to determine the calorimetric enthalpy, ΔH_{cal}, and melting temperature, T_M, as the temperature corresponding to the maximum of heat capacity.[64–67]

Pressure-Perturbation Calorimetry

PPC measurements were conducted on a MicroCal VP-DSC instrument with a PPC accessory (MicroCal, LLC, Northampton, MA) using previously described experimental protocols.[27]

High Precision Densimetry and Ultrasonic Velocimetry

All densities were measured with a precision of $\pm 1.5 \times 10^{-6}$ g cm^{-3} using a vibrating tube densimeter (DMA-5000, Anton Paar, Graz,

Austria). The partial molar volume, $V°$, of the DNA was calculated from density values using the relationship:

$$V° = \frac{M}{\rho_\circ} - \frac{(\rho - \rho_\circ)}{\rho_\circ C} \tag{6}$$

where ρ and ρ_0 are the densities of the nucleic acid solution and the neat solvent, respectively; C is the molar concentration of the nucleic acid; and M is the molecular weight of the nucleic acid.

Solution sound velocity measurements were carried out at a frequency of 7.2 MHz using the resonator method.[68,69] The analysis of the frequency characteristics of the ultrasonic resonator cells required for sound velocity measurements was conducted by a Hewlett Packard model E5100A network/spectrum analyzer (Mississauga, ON, Canada). For the type of ultrasonic resonators used in this work, the relative precision of the sound velocity measurements is about $\pm 1 \times 10^{-4}$ %.[68,70] The key characteristics of a solute directly derived from ultrasonic velocimetric measurements is the relative molar sound velocity increment, $[U] = (U - U_0)/U_0 C$, where U and U_0 are the sound velocities in the DNA solution and the neat solvent, respectively.

The values of the relative molar sound velocity increment, $[U]$, were used in conjunction with the measured partial molar volume data, $V°$, to calculate the partial molar adiabatic compressibility, $K°_S$, of the DNA from the following relationship[71,72]:

$$K°_S = \beta_{S°} \left(2V° - 2[U] - \frac{M}{\rho_\circ} \right) \tag{7}$$

where $\beta_{S°}$ is the coefficient of adiabatic compressibility of the solvent. The densimetric and ultrasonic velocimetric experiments were carried out at least in triplicate. The average values of $[U]$ and $V°$ were used in the analysis.

Densimetric and acoustic titrations were performed at 25°C following the previously described experimental protocol.[73] The titration experiments were performed by adding aliquots of a 0.2–1M potassium chloride solution to the initially potassium-free DNA solution containing tetrabutylammonium phosphate.

Computation of Solvent Accessible Surface Areas and Molecular Volumes

Our analysis is based on the NMR-determined potassium-induced G-quadruplex structure of the ODN (PDB entry 2HY9) obtained from the RCSB Protein Databank. As 2HY9 contained 10 models, each was treated as a distinct structure. We generated an unfolded single stranded structure for the ODN by first creating B-form DNA with AmberTools (v1.3) [NAB (Nucleic Acid Builder) T J. Macke, W.A. Svrcek-Seiler, R. A. Brown, I. Kolossváry, Y. J. Bomble, and D. A. Case] and then deleting the complementary strand. In order to model a more plausible single stranded structure, molecular dynamics was carried out on the single stranded structure using GROMACS (v 4.0.7).

In our simulations, the DNA molecule was contained in a rectangular box with a 40-Å distance between the solute and box sides; this system contained 55,604 water molecules and 25 potassium ions (volume: 1713.23 nm^3, density 979.409 g/L). Initially, a 100-ps steepest-descent minimization run was conducted to relax each structure [http://wwwuser.gwdg.de/~ggroenh/SaoCarlos2008/html/build.html#

top, accessed August, 2010]. A 100-ps solvent equilibration run was performed at 300 K and 1 atmosphere. Subsequently, the conformational space available to the ODN in solution was explored by running a 1-ns MD. The solvent-accessible surface area and molecular volume were calculated following these 1-ns runs. PDB "snapshots" were generated for conformations with the largest and smallest total solvent-accessible surface areas during the 1-ns simulations, which were subsequently employed in subsequent intrinsic volume and surface area calculations (see below).

We calculated the solvent-accessible surface area, S_A, for each structure as the sum of the accessible surface areas of all atoms in the structure. The intrinsic volumes, V_M, of the ODN in its G-quadruplex and coil conformations were calculated as molecular volumes as described by Richards.[44,45] Each PDB file was stripped of water molecules and cleaned using VMD (version 1.9.1) on a Linux platform. The program MSP (Molecular Surface Package) Version 3.9.3 was obtained from Dr. Michael Connolly at www.biohedron.com and used to calculate the solvent-accessible surface area and molecular volume for each structure, using a 1.4 Å probe radius on a Linux platform.

REFERENCES

1. Shafer, R. H.; Smirnov, I. Biopolymers 2000, 56, 209–227.
2. Hurley, L. H. Nat Rev Cancer 2002, 2, 188–200.
3. Huppert, J. L. Philos Trans Royal Soc A 2007, 365, 2969–2984.
4. Huppert, J. L. Chem Soc Rev 2008, 37, 1375–1384.
5. Oganesian, L.; Bryan, T. M. Bioessays 2007, 29, 155–165.
6. De Cian, A.; Lacroix, L.; Douarre, C.; Temime-Smaali, N.; Trentesaux, C.; Riou, J. F.; Mergny, J. L. Biochimie 2008, 90, 131–155.
7. Balasubramanian, S.; Hurley, L. H.; Neidle, S. Nat Rev Drug Disc 2011, 10, 261–275.
8. Dai, J. X.; Carver, M.; Yang, D. Z. Biochimie 2008, 90, 1172–1183.
9. Dai, J.; Carver, M.; Punchihewa, C.; Jones, R. A.; Yang, D. Nucleic Acids Res 2007, 35, 4927–4940.
10. Ambrus, A.; Chen, D.; Dai, J. X.; Bialis, T.; Jones, R. A.; Yang, D. Z. Nucleic Acids Res 2006, 34, 2723–2735.
11. Dai, J. X.; Punchihewa, C.; Ambrus, A.; Chen, D.; Jones, R. A.; Yang, D. Z. Nucleic Acids Res 2007, 35, 2440–2450.
12. Phan, A. T.; Luu, K. N.; Patel, D. J. Nucleic Acids Res 2006, 34, 5715–5719.
13. Luu, K. N.; Phan, A. T.; Kuryavyi, V.; Lacroix, L.; Patel, D. J. J Am Chem Soc 2006, 128, 9963–9970.
14. Xu, Y.; Noguchi, Y.; Sugiyama, H. Bioorg Med Chem 2006, 14, 5584–5591.
15. Makarov, V.; Pettitt, B. M.; Feig, M. Acc Chem Res 2002, 35, 376–384.
16. Chalikian, T. V.; Volker, J. Hydration of Nucleic Acids. In Wiley Encyclopedia of Chemical Biology, Begley, T. P., Ed.; Wiley and Sons, Inc: 2008.
17. Westhof, E. Annu Rev Biophys Biophys Chem 1988, 17, 125–144.
18. Saenger, W.; Hunter, W. N.; Kennard, O. Nature 1986, 324, 385–388.
19. Bukin, V. A. Mol Biol 1987, 21, 512–525.
20. Feig, M.; Pettitt, B. M. Biopolymers 1998, 48, 199–209.
21. Auffinger, P.; Hashem, Y. Curr Opin Struct Biol 2007, 17, 325–333.
22. Miyoshi, D.; Matsumura, S.; Nakano, S.; Sugimoto, N. J Am Chem Soc 2004, 126, 165–169.
23. Miyoshi, D.; Sugimoto, N. Biochimie 2008, 90, 1040–1051.
24. Miyoshi, D.; Karimata, H.; Sugimoto, N. J Am Chem Soc 2006, 128, 7957–7963.
25. Nagatoishi, S.; Isono, N.; Tsumoto, K.; Sugimoto, N. Chembiochem 2011, 12, 1822–1826.
26. Miller, M. C.; Buscaglia, R.; Chaires, J. B.; Lane, A. N.; Trent, J. O. J Am Chem Soc 2010, 132, 17105–17107.
27. Fan, H. Y.; Shek, Y. L.; Amiri, A.; Dubins, D. N.; Heerklotz, H.; Macgregor, R. B.;Chalikian, T. V. J Am Chem Soc 2011, 133, 4518–4526.
28. Luus, R.; Jaakola, T. H. I. AIChE J 1973, 19, 760–766.
29. Record, M. T.; Anderson, C. F.; Lohman, T. M. Q. Rev Biophys 1978, 11, 103–178.
30. Cheng, Y. K.; Pettitt, B. M. Prog Biophys Mol Biol 1992, 58, 225–257.
31. Olsen, C. M.; Gmeiner, W. H.; Marky, L. A. J Phys Chem B 2006, 110, 6962–6969.
32. Lane, A. N.; Chaires, J. B.; Gray, R. D.; Trent, J. O. Nucleic Acids Res 2008, 36, 5482–5515.
33. Mashimo, T.; Yagi, H.; Sannohe, Y.; Rajendran, A.; Sugiyama, H. J Am Chem Soc 2010, 132, 14910–14918.
34. Antonacci, C.; Chaires, J. B.; Sheardy, R. D. Biochemistry 2007, 46, 4654–4660.
35. Gray, R. D.; Buscaglia, R.; Chaires, J. B. J Am Chem Soc 2012, 134, 16834–16844.
36. Boncina, M.; Lah, J.; Prislan, I.; Vesnaver, G. J Am Chem Soc 2012, 134, 9657–9663.
37. Majhi, P. R.; Qi, J. Y.; Tang, C. F.; Shafer, R. H. Biopolymers 2008, 89, 302–309.
38. Chalikian, T. V. Annu Rev Biophys Biomol Struct 2003, 32, 207–235.
39. Chalikian, T. V. J Phys Chem B 2008, 112, 911–917.
40. Conway, B. E. J Solution Chem 1978, 7, 721–770.
41. Edward, J. T.; Farrell, P. G. Can J Chem 1975, 53, 2965–2970.
42. Kharakoz, D. P. J Solution Chem 1992, 21, 569–595.
43. Connolly, M. L. Science 1983, 221, 709–713.
44. Richards, F. M. Annu Rev Biophys Bioeng 1977, 6, 151–176.
45. Richards, F. M. Methods Enzymol 1985, 115, 440–464.
46. Till, M. S.; Ullmann, G. M. J Mol Model 2010, 16, 419–429.
47. Wang, Y.; Patel, D. J. Structure 1993, 1, 263–282.
48. Chalikian, T. V.; Totrov, M.; Abagyan, R.; Breslauer, K. J. J. Mol. Biol. 1996, 260, 588–603.
49. Imai, T.; Kovalenko, A.; Hirata, F. J Phys Chem B 2005, 109, 6658–6665.
50. Bano, M.; Marek, J. Biophys Chem 2006, 120, 44–54.
51. Patel, N.; Dubins, D. N.; Pomes, R.; Chalikian, T. V. J Phys Chem B 2011, 115, 4856–4862.
52. Patel, N.; Dubins, D. N.; Pomes, R.; Chalikian, T. V. Biophys Chem 2012, 161, 46–49.
53. Chalikian, T. V. J Phys Chem B 2001, 105, 12566–12578.

54. Chalikian, T. V.; Breslauer, K. J. Biopolymers 1998, 48, 264–280.

55. Chalikian, T. V.; Breslauer, K. J. Curr Opin Struct Biol 1998, 8, 657–664.

56. Chalikian, T. V.; Sarvazyan, A. P.; Breslauer, K. J. Biophys Chem 1994, 51, 89–107.

57. Chalikian, T. V.; Volker, J.; Srinivasan, A. R.; Olson, W. K.; Breslauer, K. J. Biopolymers 1999, 50, 459–471.

58. Chalikian, T. V.; Sarvazyan, A. P.; Plum, G. E.; Breslauer, K. J. Biochemistry 1994, 33, 2394–2401.

59. Tikhomirova, A.; Chalikian, T. V. J Mol Biol 2004, 341, 551–563.

60. Chalikian, T. V.; Macgregor, R. B. Phys Life Rev 2007, 4, 91–115.

61. Mathieson, J. G.; Conway, B. E. J Solution Chem 1974, 3, 455–477.

62. Buckin, V. A.; Kankiya, B. I.; Sarvazyan, A. P.; Uedaira, H. Nucleic Acids Res 1989, 17, 4189–4203.

63. Wilton, D. J.; Ghosh, M.; Chary, K. V. A.; Akasaka, K.; Williamson, M. P. Nucleic Acids Res 2008, 36, 4032–4037.

64. Breslauer, K. J.; Freire, E.; Straume, M. Methods Enzymol 1992, 211, 533–567.

65. Breslauer, K. J Methods Enzymol 1995, 259, 221–242.

66. Privalov, P. L.; Potekhin, S. A. Methods Enzymol 1986, 131, 4–51.

67. Privalov, G. P.; Privalov, P. L. Methods Enzymol 2000, 323, 31–62.

68. Sarvazyan, A. P. Ultrasonics 1982, 20, 151–154.

69. Eggers, F.; Funck, T. Rev Sci Instrum 1973, 44, 969–977.

70. Sarvazyan, A. P.; Chalikian, T. V. Ultrasonics 1991, 29, 119–124.

71. Barnartt, S. J Chem Phys 1952, 20, 278–279.

72. Owen, B. B.; Simons, H. L. J Phys Chem 1957, 61, 479–482.

73. Filfil, R.; Chalikian, T. V. J Mol Biol 2003, 326, 1271–1288.

74. Schweiker, K. L.; Makhatadze, G. I. Methods Enzymol 2009, 466, 527–547.

75. Lee, S.; Heerklotz, H.; Chalikian, T. V. Biophys Chem 2010, 148, 144–147.

Reviewing Editor: Kenneth J. Breslauer